Lab on a Chip

PAPER

View Article Online
View Journal

Cite this: DOI: 10.1039/c5lc00722d

Supersoft lithography: candy-based fabrication of soft silicone microstructures†

Christopher Moraes,[abc] Joseph M. Labuz,[bc] Yue Shao,[d] Jianping Fu[bd] and Shuichi Takayama*[bce]

Received 25th June 2015,
Accepted 29th July 2015

DOI: 10.1039/c5lc00722d

www.rsc.org/loc

We designed a fabrication technique able to replicate microstructures in soft silicone materials ($E < 1$ kPa). Sugar-based 'hard candy' recipes from the confectionery industry were modified to be compatible with silicone processing conditions, and used as templates for replica molding. Microstructures fabricated in soft silicones can then be easily released by dissolving the template in water. We anticipate that this technique will be of particular importance in replicating physiologically soft, microstructured environments for cell culture, and demonstrate a first application in which intrinsically soft microstructures are used to measure forces generated by fibroblast-laden contractile tissues.

Introduction

The ability to engineer microstructures at the length scale of cells and tissues has played an important role in understanding how biological cells interact mechanically with their environment.[1,2] Matrix mechanics are emerging as important regulators of development, homeostasis, and disease in various biological systems. Hence, recapitulating the stiffness of tissues (Young's modulus $E \approx$ 0.1–100's of kPa) *in vitro* is now considered an important strategy in tissue engineering, regenerative medicine, and fundamental studies of cell biology.[3] However, 'soft lithography', the primary enabling technology in fabricating micron-scale structures is typically limited to supraphysiologically stiff elastomeric materials such as conventional polydimethylsiloxane (PDMS; $E \approx$ 1000 kPa), and is challenging to apply when working with very soft materials. Here, we leverage techniques originating in the confectionery industry to develop 'supersoft lithography', a simple, robust, and versatile approach to replicate microstructures in soft silicone materials ($E \approx$ 0.1 kPa). We then apply this approach towards fabricating soft PDMS templates capable of measuring both long-term and real-time contractile forces generated by toroid-shaped engineered microtissues.

Existing methods to microfabricate intrinsically soft microstructures suffer some severe limitations. Both top-down techniques such as microscale laser machining, and bottom-up printing and photopatterning techniques are expensive, require specialized equipment, and/or are challenging to scale up device production.[4] Replica molding presents a viable alternative to these strategies, and has to date been applied to microfabricate structures in soft hydrogel materials such as collagen,[5–8] polyacrylamide,[9–11] and polyethylene glycol.[12,13] However, use of these low-toughness materials limits the vertical dimensions of these fabricated structures, due to challenges in mechanically removing the template from the hydrogel. As such, previous studies with these approaches have been limited to working with feature thicknesses of tens of microns, and feature resolutions of several hundred microns.[9] Furthermore, hydrogels undergo large degrees of stiffness-dependent swelling,[9,14] up to 1200% for very soft gels,[14] making it challenging to replicate high-fidelity microscale features in soft materials. In contrast, soft silicones such as Sylgard 527 (Dow Corning, $E \approx$ 1 kPa) exhibit low shrinkage/swelling ratios in aqueous medium,[15–20] and can be blended with conventional Sylgard 184 to match stiffnesses across the physiological range.[21] Our measurements of baseline Sylgard 527 stiffness by shear rheometry indicates that with a monomer : crosslinker ratio of 1 : 1, Sylgard 527 has a Young's modulus of 1.5 kPa, three orders of magnitude less than conventional Sylgard 184 PDMS (Fig. 1A). This material modulus varied by <0.1 kPa over strains up to 250% (Fig. 1B). The modulus was further reduced to <0.1 kPa when the component ratios were altered by a very small degree (5 : 4; Fig. 1A), and exhibited no measurable change at high strains (Fig. 1A and B).

[a] Department of Chemical Engineering, McGill University, 3610 University Street, Montreal, QC H3A 2B2, Canada
[b] Department of Biomedical Engineering, College of Engineering, University of Michigan, 2200 Bonisteel Blvd, Ann Arbor, MI 48109, USA.
E-mail: takayama@umich.edu
[c] Biointerfaces Institute, University of Michigan, NCRC, 2800 Plymouth Road, MI 48109-2800, USA
[d] Department of Mechanical Engineering, University of Michigan, Ann Arbor, Michigan 48109, USA
[e] Macromolecular Science and Engineering Center, College of Engineering, University of Michigan, 2300 Hayward St., Ann Arbor, MI 48109, USA
† Electronic supplementary information (ESI) available. See DOI: 10.1039/c5lc00722d

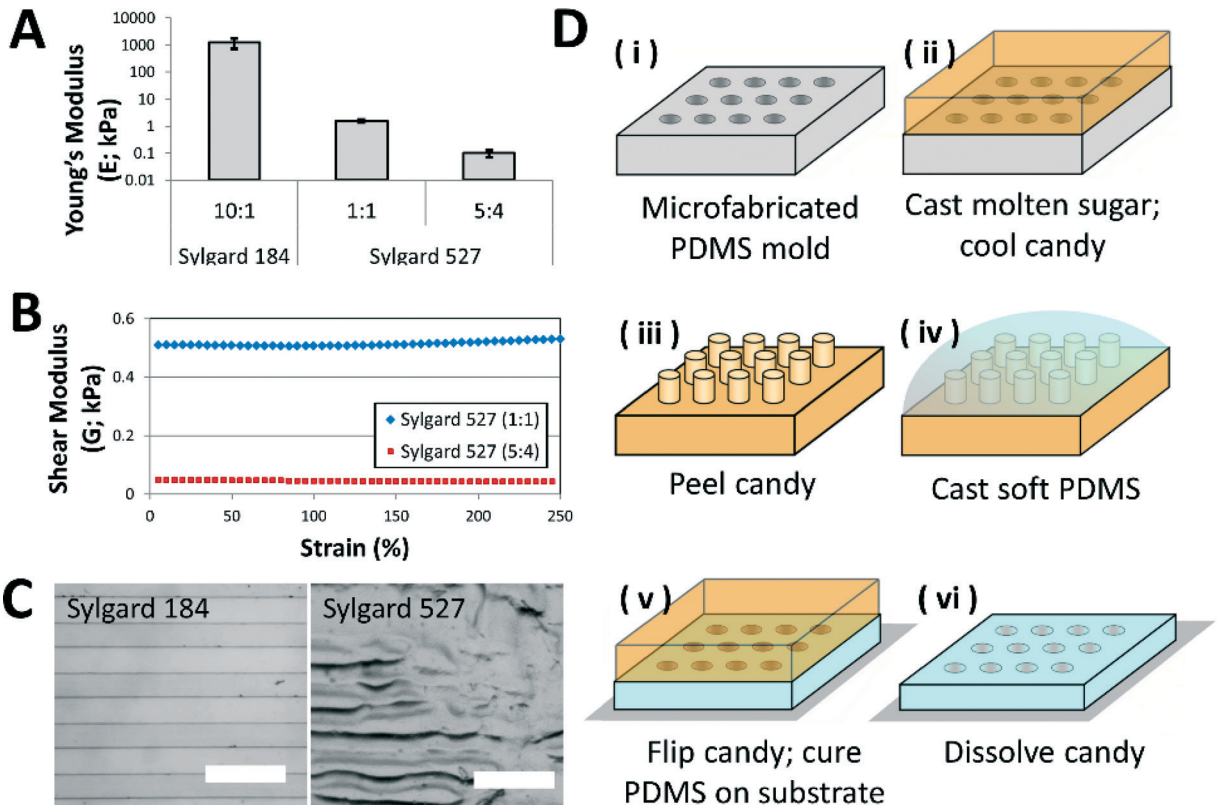

Fig. 1 (A) Comparison between mechanical properties of conventional PDMS (Sylgard 184), and soft PDMS (Sylgard 527) in the prescribed 1 : 1 ratio and a modified 5 : 4 ratio. Soft PDMS is three to four orders of magnitude more compliant than conventional PDMS. (B) The shear modulus of soft PDMS does not deviate significantly from the baseline over 300% applied strain, as assessed by shear rheometry. (C) Microfabricating conventional PDMS is simple, but applying similar processes to soft PDMS yields microstructures of poor fidelity, due to large deformations that occur during the peeling step of removing the silicone polymer from the master. Scale bar = 300 μm. (D) Proposed fabrication process to microfabricate soft structures in PDMS. (i) A conventional PDMS mold is degassed and (ii) serves as a template against which the molten sugar solution is cast and allowed to cool. (iii) The candy with microstructured features in the surface is peeled from the PDMS mold and (iv) used as a mold for soft PDMS. (v) The soft PDMS is cured at 60 °C overnight between the candy and a rigid substrate. (vi) The candy is then dissolved in warm water, releasing the microfabricated soft PDMS layer.

Fabricating microstructures in soft PDMS using the standard soft lithography replica molding technique proved challenging. In contrast with demolding 40 μm-deep channel features in conventional Sylgard 184 (Fig. 1C, left panel), features in Sylgard 527 (Fig. 1C, right panel) ripped and smeared during peeling, despite silanization of the mold structure and use of ethanol as a de-molding agent. To enable mold release, we developed a sacrificial template material that can be completely dissolved away. Sacrificial materials have previously been applied to create soluble surface coatings,[22,23] but these materials cannot be easily applied to structures taller than ~10 μm,[22] and cannot be used as bulk templates without significant cracking and feature distortion. In this work, we develop a hard sugar-based sacrificial material for fabrication of bulk microstructured templates. Although sugar-based sacrificial materials have been used to release surface structures,[22] fabricate porous PDMS materials[24–26] and engineer vascularized tissues,[27,28] these previous works were not concerned with high-fidelity pattern replication in PDMS. Here, we modify water-soluble candy to be mechanically rigid, heat resistant, and capable of replicating high-resolution microstructures. Soft PDMS is cured on these candy molds, and then released by immersing the sample in water (Fig. 1D).

Design of sacrificial sugar materials

Our first attempts at designing the sacrificial candy material followed standard recipes from the confectionery industry (ESI†). Cooking a mixture of water, corn syrup, sugar and acetic acid converts the sucrose to glucose and fructose, while the dextroses and monosaccharides present in corn syrup prevent crystallization of the candy. Once the mixture is cooked to the 'hard-crack stage' (150 °C), and there is less than 2% of water remaining in the solution, it cools to form a brittle glass,[29] similar to the 'breakaway glass' used in Hollywood stunt sequences.

Mechanical characterization of the inverted sugar candy revealed that the material has a low glass transition temperature (T_g; Fig. 2A). Curing at elevated temperatures therefore distorts the microfeatures. Furthermore, we found that our attempts at room temperature cures over 24–48 hours also resulted in poor feature fidelity (ESI,† Fig. S1), likely because sugar-based materials are susceptible to humidity, which

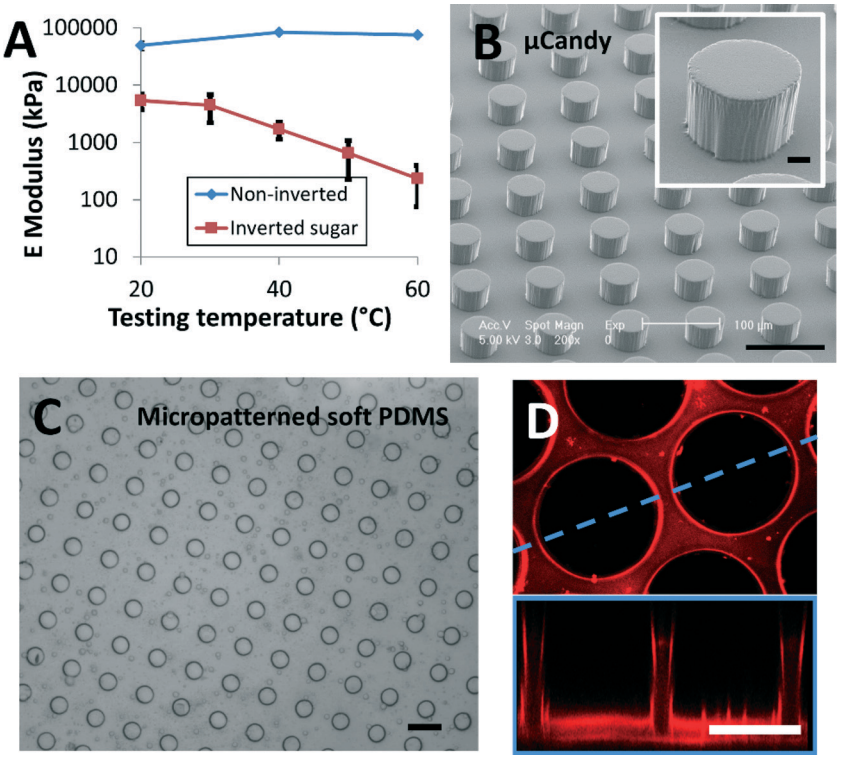

Fig. 2 Characterization of the supersoft lithography process. (A) Modulus of candy fabricated with the conventional inverted sugar process (red line) and the non-inverted sugar process (blue line) as a function of temperature. The inverted sugar process produces candy with a low glass transition temperature, making it unsuitable for supersoft lithography. In contrast, the non-inverted sugar maintained rigidity over the range of temperatures necessary to process PDMS. (B) Scanning electron microscopy reveals that candy cast against PDMS templates retains microscale features on release (scale bar = 100 μm, inset scale bar = 10 μm). (C) Patterns transferred into soft PDMS of modulus 1.5 kPa. Scale bar = 100 μm, and (D) deep microwells patterned into softer PDMS of modulus 0.1 kPa, and imaged using confocal microscopy of surface adsorbed fluorescent dye. Top panel = plan view, blue dashed line = cut-section shown in bottom panel (side view). Scale bar = 400 μm.

causes feature degradation over extended time periods. For example, cotton candy (similar to our material) completely collapses within 6 hours at 45% humidity.[30] Furthermore, these numbers reflect bulk material changes, and surface damage of microfeatures is likely to occur much more rapidly. Hence, to circumvent humidity-driven template degradation, rapid (and therefore, high temperature) curing protocols are required. Raising the cure temperature to 60 °C would also reduce relative humidity by 85% (assuming a baseline indoor humidity of 50%). This temperature difference would therefore drive an ~100% decrease in sugar moisture content,[31] and a corresponding 100× increase in template rigidity.[29] Hence, optimizing the temperature resistance of the candy templates is of critical importance in the success of this technique.

To increase T_g, we minimized the amount of sucrose inverted by maintaining a neutral pH, and sped up cook times. Sugar and light corn syrup in a 2 : 1 w/w ratio were microwaved until the sugar caramelized. Cook time varies depending on microwave power, and so the process was monitored by observing color changes from clear to brown and the distinct aroma of caramelizing sugar. These measures reduce T_g by minimizing the glucose and fructose monosaccharides in the candy.[32] Since extended caramelization is known to raise T_g by polymerizing monosaccharide molecules,[33] all samples were caramelized to a medium-brown color (ESI† Fig. S2). The non-inverted candy had significantly improved mechanical rigidity and a $T_g > 60$ °C (Fig. 2A), making it suitable for PDMS processing.

Fabrication of soft silicone microstructures

The molten sugar was cast against a Sylgard 184 PDMS mold containing microfabricated features. Candy pucks containing microfabricated features could be peeled from the PDMS mold, and were then stored in a vacuum desiccator until use. The supersoft lithography process is best performed in low-humidity environments, as the candy is hygroscopic and loses feature fidelity on exposure to moisture. Scanning electron microscopy (SEM) analysis of the replicated sugar indicated that microscale features were transferred into and maintained in the candy (Fig. 2B). No features were detected on the flat portions of the sugar mold, and minor nanoscale roughness present in the sidewalls of the SU-8 master were faithfully replicated. To demonstrate the versatility of this technique for even smaller structures, arrays of micron-scale posts were also faithfully replicated and maintained in the candy (ESI,† Fig. S3).

Using this process, microfeatures were easily transferred from the candy molds into the Sylgard 527 PDMS (Fig. 2C;

E = 1.5 kPa) with feature resolutions down to 20 μm (ESI,† Fig. S1). Furthermore, tall microstructures (>400 μm) were fabricated in even softer PDMS (Fig. 2D; E = 0.1 kPa), although working with such soft materials was challenging as the soft structures collapse easily (ESI,† Fig. S4).

Application: measuring microtissue forces

As a first biological application of this technology, we developed intrinsically soft features to measure the mechanical forces exerted during contractile tissue formation. The forces involved in tissue remodeling are crucial features of development and morphogenesis, and previous approaches by Legant *et al.*, measured these by developing microfabricated PDMS cantilevers that tether a contractile dog-bone shaped microtissue.[34] The effective stiffness of the cantilever is reduced by decreasing the geometric cross-section of the cantilever, enabling the measurement of small contractile forces. Although extremely useful,[35,36] the dog-bone shaped tissues may exhibit strong necking profiles[37] leading to varied cross-sectional areas, and thus, significant variations in internal tissue stresses.

To address this issue, we used the supersoft lithography process to fabricate 400 μm tall pillar structures in soft Sylgard 527 PDMS, which were fluorescently labelled and around which toroid-shaped microtissues of uniform cross-section can be formed (Fig. 3A). Contraction of microtissues by a model stromal fibroblast cell line (HS-5; ATCC) generated compressive mechanical forces on the central pillar.

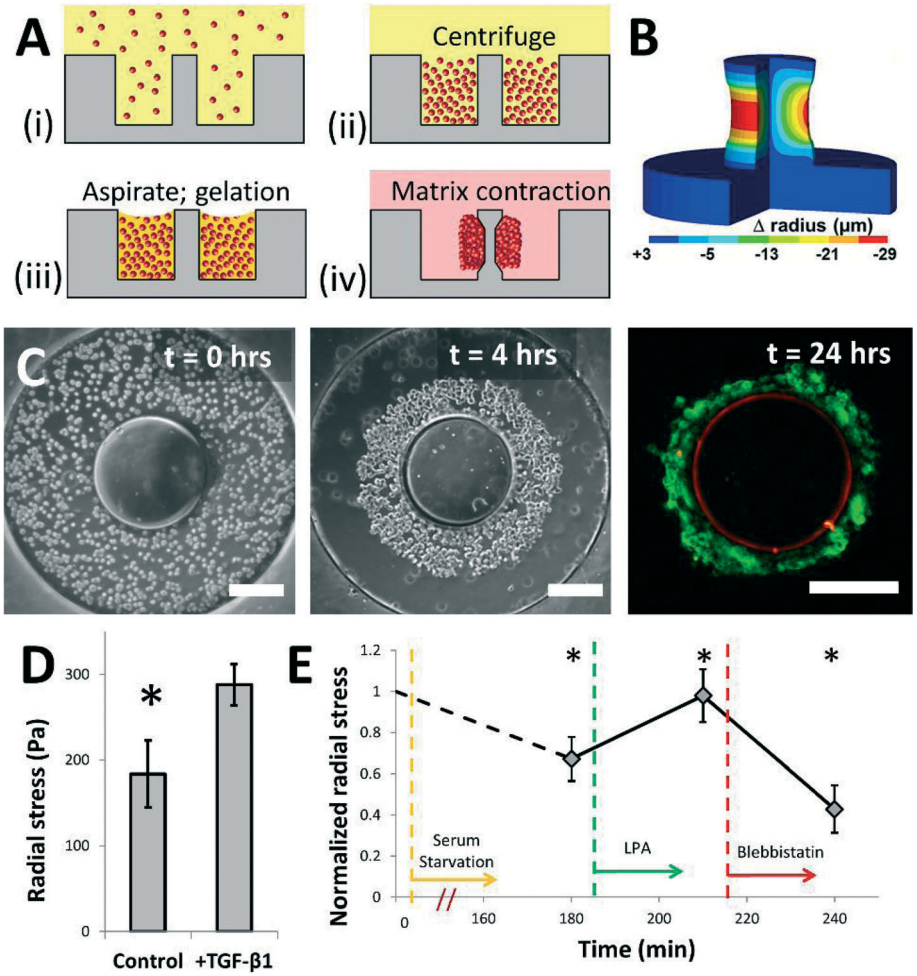

Fig. 3 Microstructured pillars in soft PDMS were designed to measure contractile forces generated by a toroid-shaped microtissue. (A) Microtissue fabrication and contraction process workflow: (i) a neutralized collagen gel solution containing cells is dispensed into the toroid-shaped chambers, and (ii) centrifuged to drive the cells into the chamber. (iii) Excess collagen is aspirated, and the remaining solution is allowed to polymerize at 37 °C. (iv) Cell culture media is replaced and the collagen matrix is allowed to contract. (B) Changes in pillar radius are related to applied radial stress *via* finite element analysis. (C) Toroid-shaped microtissues form over a period of 24 hours, creating a band of collagen around the central micro-pillar structure. (red = DiI-stained PDMS, green = cellular actin; scale bars = 200 μm). (D) The presence of soluble factors such as TGF-β1 during the tissue maturation process increases stresses generated by the toroidal microtissues (* $p < 0.001$, n = 13–15). (E) Starving the cells of serum for 3 hours reduces microtissue-generated radial stresses. Adding lysophosphatidic acid (LPA, 10 μg mL^{-1}) increased stress generation to pre-starvation levels, and adding blebbistatin (50 μM) to inhibit myosin II activity reduced stresses by 60% (* $p < 0.001$ against the previous treatment in the time-course, n = 15), demonstrating the ability to monitor real-time stresses using this fabricated platform.

Along with finite element simulations, measuring the radial deformation of the pillar (Fig. 3B, ESI† Fig. S5) allowed quantification of the radial stresses exerted by the contracting collagen toroid. In addition to eliminating any internal stress variations in the microtissues, this approach simplifies the fabrication process eliminating the need for the multilayer overhanging PDMS tethering structures required by Legant *et al.* to hold the microtissues in place.

Finite element simulations of the contractile tissue band around the pillar indicated that the change in radius of the pillar under applied loads was linearly related to the applied radial stresses. Interestingly, normalizing the change in radius to the initial radius of the pillar revealed that the sensitivity of the stress measurement decreased with increasing pillar diameter, due to the asymmetric boundary constraints above and below the contractile tissue band on the micropillar (ESI† Fig. S5). Since the gain in sensitivity does not improve substantially when the pillar radius is reduced below 200 μm, all further experiments were conducted with this pillar geometry.

The collagen underwent remodeling over a period of 24 h to form a tight ring around the deformable central pillar (Fig. 3C). While cell-free collagen microtissues did not cause a measurable change in pillar diameter (data not shown), contractile microtissues deformed the pillar, as shown *via* the overlaid images of the base- and mid-points of a representative experiment (ESI† Fig. S6B). Control experiments demonstrate no measurable deformation of the pillar when using 'hard' Sylgard 184 PDMS (ESI† Fig. S6C). To account for any post-to-post variation due to minor shrinkage/swelling of the PDMS or collagen biomaterial, all further measurements were made by normalizing the diameter of the pillar immediately after microtissue formation, with the diameter of the pillar at the time of interest.

As expected, microtissues responded to soluble factors in the medium. Culture with 5 ng mL^{-1} transforming growth factor (TGF)-β1 significantly increased the radial stresses generated during collagen contraction (Fig. 3D), consistent with previously published reports.[36,38] To demonstrate real-time measurements of microtissue force generation using this platform, serum starvation conditions were used to reduce the radial contractile forces by approximately 30% over 3 h, and the addition of lysophosphatidic acid (LPA), a stimulant of myosin activity, restored contractile forces to pre-starvation levels within 30 min. Inhibiting the cellular myosin ATPase machinery with Blebbistatin (50 μM; Enzo Life Sciences) reduced radial stresses by over 60%. The remodeled collagen continued to exert static radial stresses, which prevented complete relaxation of the central pillar, demonstrating these supersoft structures are indeed capable of sensing forces generated by microengineered tissues (Fig. 3E).

Conclusions

We have developed a technique to generate microstructures in very soft silicone materials with bulk modulus E down to 0.1–1 kPa, and demonstrated the applicability of this technology by developing intrinsically soft sensing pillars to measure contractile tissue forces. We designed the supersoft lithography process to be easily adopted into microfabrication labs, as it is extremely simple, cost-effective, reliable, and once the initial silicon mold is produced does not require specialized equipment or expertise. More broadly, we expect that this supersoft lithography approach will enable the integration of soft materials into microfabricated systems, improving the relevance, applicability, and potential for such devices to probe biological systems.

Methods

Supersoft lithography

Candy ingredients were purchased off the shelf at a local supermarket. Karo light corn syrup and table sugar were mixed in a 1 : 2 v/v ratio and microwaved until caramelized. The molten sugar was poured over degassed PDMS templates, and placed under vacuum to remove trapped bubbles. If the sample solidified too quickly, it was re-heated in the microwave. Cooled samples were easily peeled from the PDMS template. Sylgard 527 (Dow Corning) components were mixed in the specified ratio, cast on the sugar molds and degassed under vacuum. Separate samples of the cured PDMS were mechanically characterized as outlined in ESI.† Candy molds were then inverted and placed in a Petri dish, sandwiching the pre-polymerized PDMS between the tissue culture plastic and the sugar mold. Devices were cured in an oven at 60 °C overnight with dessicant to minimize humidity. The plates were then soaked in a large container of water on a shaker plate for 2 hours to dissolve the sacrificial candy mold. Devices were washed with distilled water, and incubated at room temperature for 1 hour with 5 μg mL^{-1} DiI (Invitrogen) to fluorescently label the PDMS surface, and for 1 hour with 1% Pluronic F-108 (BASF) to prevent surface protein adhesion.

Collagen microtissue formation

For cell culture protocols, see ESI.† Collagen solution was prepared by mixing 10% 10× DMEM, Type I collagen (bovine, BD Biosciences) and sterile water, and neutralized with NaOH. Cell suspensions were added to dilute the collagen to 2 mg mL^{-1}, and to realize ~200–400 cells per cavity after centrifugation. The collagen solution was overlaid on the devices, mixed thoroughly, and centrifuged in a plate-bucket holder at 200 RCF for 2 minutes at 4 °C. Excess collagen was then aspirated. The collagen microtissues were polymerized in a humidified incubator (37 °C, 5% CO_2) for 30 minutes, and then imaged to establish baseline pillar diameters immediately following microtissue formation. Fully-supplemented media was then added to the devices to enable cell growth, with or without the following supplements for specific experiments: transforming growth factor (TGF)-β1 (5 ng mL^{-1}; Peprotech), lysophosphatidic acid (LPA, 10 μg mL^{-1}; Cayman Chemical), blebbistatin (50 μM, Enzo Life Sciences).

Image collection and statistics

Scanning electron microscopy images were collected on a Philips XL30 FEG. Fluorescent images were collected using either a confocal (Nikon A1) or epifluorescent (Nikon TE300) inverted microscope with a 20× objective. All image analysis was performed in ImageJ (see ESI†). All data reported as means ± standard deviation. Statistical analysis conducted by ANOVA in SigmaStat 3.5 (Systat Software Inc.; San Jose, CA, USA). The Tukey method was used for *post-hoc* comparisons.

Acknowledgements

We thank Youngri Kim and Michael Solomon for technical assistance with shear rheometry measurements; and Gary Luker for the gift of HS-5 cells. We gratefully acknowledge support from the Natural Sciences and Engineering Research Council of Canada, and the Banting postdoctoral fellowship programs to CM, and US Department of Education GAANN and NIH MBSTP (NIH T32 EB005582) fellowships to JML. This work was supported by the NSF (CBET 1149401 to JF) and NIH (CA 170198 and AI116482 to ST).

References

1 Kshitiz, P. Park, W. Kim, A. J. Helen, A. Engler, A. Levchenko and D.-H. Kim, *Integr. Biol.*, 2012, **4**, 1008–1018.
2 C. Moraes, Y. Sun and C. A. Simmons, *Integr. Biol.*, 2011, **3**, 959–971.
3 F. M. Watt and W. T. S. Huck, *Nat. Rev. Mol. Cell Biol.*, 2013, **14**, 467–473.
4 M. L. McCain, A. Agarwal, H. W. Nesmith, A. P. Nesmith and K. K. Parker, *Biomaterials*, 2014, **35**(21), 5462–5471.
5 M. D. Tang, A. P. Golden and J. Tien, *J. Am. Chem. Soc.*, 2003, **125**, 12988–12989.
6 C. M. Kraning-Rush, S. P. Carey, M. C. Lampi and C. A. Reinhart-King, *Integr. Biol.*, 2013, **5**, 606.
7 C. M. Nelson, M. M. VanDuijn, J. L. Inman, D. A. Fletcher and M. J. Bissell, *Science*, 2006, **314**, 298–300.
8 Y. Zheng, P. W. Henderson, N. W. Choi, L. J. Bonassar, J. A. Spector and A. D. Stroock, *Biomaterials*, 2011, **32**, 5391–5401.
9 J. M. Charest, J. P. Califano, S. P. Carey and C. A. Reinhart-King, *Macromol. Biosci.*, 2012, **12**, 12–20.
10 S. Al-Haque, J. W. Miklas, N. Feric, L. L. Y. Chiu, W. L. K. Chen, C. A. Simmons and M. Radisic, *Macromol. Biosci.*, 2012, **12**, 1342–1353.
11 C. M. Kraning-Rush and C. A. Reinhart-King, *Cell Adh. Migr.*, 2012, **6**, 274–279.
12 K. Y. Suh, J. Seong, A. Khademhosseini, P. E. Laibinis and R. Langer, *Biomaterials*, 2004, **25**, 557–563.
13 S. Kobel, M. Limacher, S. Gobaa, T. Laroche and M. P. Lutolf, *Langmuir*, 2009, **25**, 8774–8779.
14 A. Buxboim, K. Rajagopal, A. E. X. Brown and D. E. Discher, *J. Phys.: Condens. Matter*, 2010, **22**, 194116.
15 C. Moraes, Y. Sun and C. A. Simmons, *J. Micromech. Microeng.*, 2009, **19**, 065015.
16 B. Trappmann, J. E. Gautrot, J. T. Connelly, D. G. T. Strange, Y. Li, M. L. Oyen, M. A. C. Stuart, H. Boehm, B. Li, V. Vogel, J. P. Spatz, F. M. Watt and W. T. S. Huck, *Nat. Mater.*, 2012, **11**, 642–649.
17 Y. Sun, K. M. A. Yong, L. G. Villa-Diaz, X. Zhang, W. Chen, R. Philson, S. Weng, H. Xu, P. H. Krebsbach and J. Fu, *Nat. Mater.*, 2014, **13**, 599–604.
18 Y. Sun, L.-T. Jiang, R. Okada and J. Fu, *Langmuir*, 2012, **28**, 10789–10796.
19 M. Mayer, R. Rabindranath, J. Borner, E. Horner, A. Bentz, J. Salgado, H. Han, H. Bose, J. Probst, M. Shamonin, G. J. Monkman and G. Schlunck, *PLoS One*, 2013, **8**, e76196.
20 S. Calve and H.-G. Simon, *FASEB J.*, 2012, **26**, 2538–2545.
21 R. N. Palchesko, L. Zhang, Y. Sun and A. W. Feinberg, *PLoS One*, 2012, **7**, e51499.
22 V. Linder, B. D. Gates, D. Ryan, B. A. Parviz and G. M. Whitesides, *Small*, 2005, **1**, 730–736.
23 J. M. Goffin, P. Pittet, G. Csucs, J. W. Lussi, J. J. Meister and B. Hinz, *J. Cell Biol.*, 2006, **172**, 259–268.
24 A. D. Lantada, H. A. Inesta, B. P. Sanchez and J. P. Garcia-Ruiz, *Adv. Mater. Sci. Eng.*, 2014, **2014**, e612976.
25 M. G. King, A. J. Baragwanath, M. C. Rosamond, D. Wood and A. J. Gallant, *Procedia Chem.*, 2009, **1**, 568–571.
26 S.-J. Choi, T.-H. Kwon, H. Im, D.-I. Moon, D. J. Baek, M.-L. Seol, J. P. Duarte and Y.-K. Choi, *ACS Appl. Mater. Interfaces*, 2011, **3**, 4552–4556.
27 L. M. Bellan, S. P. Singh, P. W. Henderson, T. J. Porri, H. G. Craighead and J. A. Spector, *Soft Matter*, 2009, **5**, 1354.
28 J. S. Miller, K. R. Stevens, M. T. Yang, B. M. Baker, D.-H. T. Nguyen, D. M. Cohen, E. Toro, A. A. Chen, P. A. Galie, X. Yu, R. Chaturvedi, S. N. Bhatia and C. S. Chen, *Nat. Mater.*, 2012, **11**, 768–774.
29 R. W. Hartel and A. Hartel, *Candy Bites*, Springer New York, New York, NY, 2014.
30 K. M. Leinen and T. P. Labuza, *J. Zhejiang Univ., Sci., B*, 2006, **7**, 85–89.
31 J. E. Maudru and T. E. Paxson, *Proc. Am. Soc. Sugar Beet*, 1950, 6.
32 J.-A. Seo, S. J. Kim, H.-J. Kwon, Y. S. Yang, H. K. Kim and Y.-H. Hwang, *Carbohydr. Res.*, 2006, **341**, 2516–2520.
33 B. Jiang, Y. Liu, B. Bhandari and W. Zhou, *J. Agric. Food Chem.*, 2008, **56**, 5138–5147.
34 W. R. Legant, A. Pathak, M. T. Yang, V. S. Deshpande, R. M. McMeeking and C. S. Chen, *Proc. Natl. Acad. Sci. U. S. A.*, 2009, **106**, 10097–10102.
35 R. Zhao, C. S. Chen and D. H. Reich, *Biomaterials*, 2014, **35**, 5056–5064.
36 A. R. West, N. Zaman, D. J. Cole, M. J. Walker, W. R. Legant, T. Boudou, C. S. Chen, J. T. Favreau, G. R. Gaudette, E. A. Cowley and G. N. Maksym, *Am. J. Physiol.*, 2013, **304**, L4–L16.
37 H. Wang, A. A. Svoronos, T. Boudou, M. S. Sakar, J. Y. Schell, J. R. Morgan, C. S. Chen and V. B. Shenoy, *Proc. Natl. Acad. Sci. U. S. A.*, 2013, 201313662.
38 C. Moraes, A. B. Simon, A. J. Putnam and S. Takayama, *Biomaterials*, 2013, **34**, 9623–9631.

